NASA TECHNICAL MEMORANDUM

NASA TM X-67934

NASA TM X-67934

PEAK AXIAL-VELOCITY DECAY WITH MIXER-TYPE EXHAUST NOZZLES

by D. Groesbeck, R. Huff, and U. von Glahn
Lewis Research Center
Cleveland, Ohio
September, 1971

This information is being published in preliminary form in order to expedite its early release.

PEAK AXIAL-VELOCITY DECAY WITH MIXER-TYPE EXHAUST NOZZLES

by

D. Groesbeck, R. Huff and U. von Glahn

INTRODUCTION

This report summarizes the preliminary results of an experimental study, conducted at the NASA Lewis Research Center, on the peak axial-velocity decay obtained with circular and non-circular nozzles and several mixer-type nozzles. Prime applications of nozzles having a rapid axial velocity decay are for (1) reduction of jet exhaust-deflected flap interaction noise associated with STOL aircraft using an externally blown flap lift augmentation system (ref. 1), (2) VTOL downwash suppression resulting from vertically oriented exhaust nozzles (refs. 2 and 3) and (3) conventional exhaust noise suppressors with and without ejectors.

A mixer-type nozzle is defined herein as consisting of multi-elements rather than a single nozzle. With a multi-element nozzle, the velocity of the individual small jets decays rapidly by mixing with the surrounding air, as shown schematically in figure 1. At some distance downstream of the nozzle exit plane, the individual jets coalesce sufficiently to form a large diameter coalescing core and a very slow peak-velocity degradation occurs. Once the coalesced core has fully formed, rapid mixing again occurs with an associated rapid velocity degradation.

APPARATUS

The test stand used in the present work is shown in figure 2. Pressurized air at about 289 K is supplied to a 15.25-cm diameter plenum by twin diametri-

cally opposed supply lines. Flexible couplings in each of the twin supply lines isolate the supply system from a force measuring system. The plenum is free to move axially through an overhead cable suspension system. A load cell at the upstream end of the plenum is used to measure thrust. The test nozzles were attached to a flange at the downstream end of the plenum.

Airflow through the overhead main supply line was measured with a calibrated orifice. The nominal nozzle inlet total pressure was measured with a single probe near the plenum exit flange.

Free jet surveys were made with a traversing pitot-static probe at several downstream stations (up to about 50-cm) from the test nozzle exit planes. Thereafter, a single pitot-static probe located on the approximate centerline of the nozzle was used at downstream distances up to 300 cm.

The measurements from the traversing probe were transmitted to an x-y-y' plotter which yielded direct traces on graph paper of the total and static pressure distribution across the jet. All other pressure data were recorded from multitube water or mercury manometers.

CONFIGURATIONS

Peak axial velocity degradation data were obtained with single-element nozzles that included the following cross sections: circular, trapezoidal, triangular and rectangular. The studies included variations in nozzle aspect ratio and nozzle area.

Multi-element nozzles included multitubes (up to 19 tubes) and multi-lobe nozzles (up to 12 lobes). The spacing between elements and circumferential rings of elements (for multitube nozzles) were studied to evaluate these

geometry effects on peak axial-velocity degradation. Typical multi-element nozzles are shown in figure 3. Pertinent dimensions for all nozzles tested are summarized in Table I.

RESULTS

Single-Element Nozzles

It was established early in the study that the peak axial-velocity degradation for single-element nozzles could be obtained using orifices rather than resorting to convergent nozzles or tubular nozzles by the use of an effective nozzle or orifice coefficient, C_e. (All symbols are defined in the appendix.) Consequently, most of the single-element nozzle configuration data were obtained using square-edge orifices and normalized by use of this coefficient as noted in the subsequent data representations.

It was also determined that the peak axial velocity degradation could be correlated in terms of U/U_j as a function of $X(C_e D_e \sqrt{1+M_j})^{-1}$.

Circular nozzles. - Peak axial velocity decay curves for circular nozzles (and orifices) are shown in figure 4. In figure 4(a) it is shown that the term $\sqrt{1+M_j}$ correlates data obtained at various jet exit Mach numbers. Consequently, although the present study covered jet exit Mach numbers from 0.46 to 1.15, it is sufficient to plot data for only a representative jet exit Mach number to establish a velocity decay curve. In figure 4(b), a comparison is made to show that square-edge orifice data correlates with tube and round-edge orifice data by including an orifice coefficient, C_e, in the abscissa parameter.

Non-circular nozzles. - The peak axial-velocity decay for non-circular nozzles (and orifices) is shown in figures 5 to 8. It is apparent in figures

5 to 7 that increasing the aspect ratio of the nozzle geometry increases the initial rate of velocity decay.

MULTI-ELEMENT NOZZLES

In this section data for multi-element nozzles consisting effectively of a single ring will be presented first, followed by data for multi-ring, multi-tube configurations.

Single-Ring Nozzles

Circular tubes. - In figure 9, the peak axial-velocity decay for a 6-tube nozzle is shown for several spacing ratios. It is apparent that with decreasing spacing ratio, the coalescing core occurs at increasing values of U/U_j.

Trapezoidal nozzles. - In figure 10, data for three square-ended trapezoidal nozzles (all having the same total area) are presented showing the effect of element spacing and element number on the velocity decay. Increasing the number of elements (constant radial height) while maintaining the spacing ratio caused an increase in the value of U/U_j. Increasing the spacing ratio (by increasing the element radial height and reducing its width) caused a decreased value of U/U_j for the same number of elements.

In figure 11, the peak axial-velocity decay for three round-ended, trapezoidal nozzles is shown. In order to extend the stay in the single-element decay region, alternate nozzles for the 8-element configuration were canted 10° outward from the overall nozzle centerline. The results of canting the alternate elements are shown in figure 12; the velocity decay was improved by a $\Delta U/U_j$ of about 0.12 over that for the uncanted elements.

Finally, the data for a 12-lobe (triangular-elements) nozzle and a 4-slot (rectangular-elements) nozzle (refs. 2 and 3, respectively) are shown in figure 13 in terms of the parameters used herein.

Coplanar Multi-Ring Nozzles

Multitube nozzles with 2 rings of tubes and with and without a tube on the overall nozzle centerline were also studied.

In figure 14, data for a 2-ring multitube nozzle without a center element is shown. It is apparent that the addition of the second tube-ring caused an earlier departure of the coalescing core from the single-element decay curve resulting in a higher U/U_j value at the departure point. An increase in the number of tubes from 6 to 12 in the outer tube ring caused a further increase in the value of U/U_j at the departure point.

Data for 2-ring multitube nozzles with an element on the nozzle centerline are shown in figure 15. In general, the velocity decay data are similar to those without the use of a center element (figs. 9 and 14); however, the departure point of the coalescing core from the single-element decay curve is at significantly higher values of U/U_j for comparable tube spacings and the same number of tubes in a given tube ring.

Non-Coplanar Multi-Ring Nozzles

A number of nozzles representing bypass-type (positive-stagger) configurations in which the core exhaust plane was located axially downstream from a secondary exhaust plane were also evaluated for peak axial velocity decay characteristics.

In figure 16, the peak velocity decay for an 8-tube core, 8-orifice bypass nozzle is shown. It should be noted that the core predominated with

respect to establishing the decay curve; thus the D_e in the abscissa of figure 16 is that for a single element of the core tubes and X is measured from the core nozzle exit plane. As in the case of the coplanar multitubes, the second ring of elements caused a significant increase in the value of U/U_j at the departure point from the single-element curve. A reduction of the secondary (bypass) jet velocity with respect to that for the core jet lowered the value of U/U_j somewhat at the departure point. These data were obtained with a plug between the core tubes (see Table I). Elimination of the plug did not affect the departure point and only slightly increased (less negative) the slope of the coalescing core curve.

In figure 17 a comparison of a 3-tube core and an 8-tube core configuration, both with an 8-orifice secondary nozzle is shown. The use of a smaller number of larger core tubes causes an increase in the value of U/U_j at the departure point compared with the data for the larger number but smaller core tube configuration. This trend is the opposite of that shown in figure 10 for trapezoidal multi-element nozzle. The trend reversal is due to the larger spacing between elements of the 8-tube nozzle compared with the 3-tube nozzle (see Table I).

In figure 18 a comparison of 3- and 8-tube core nozzles both with an annular secondary (bypass) nozzle is shown. It is apparent that with equal bypass and core velocities the value of U/U_j at the point of departure from the single core tube curve is markedly greater than that for a U_b/U_c value of 0.7.

CONCLUDING REMARKS

In the design of a multi-element mixer nozzle that is to achieve a desired peak axial-velocity ratio at a fixed distance from the nozzle exit plane, the number and spacing of multi-elements may result in an overall nozzle diameter that could be detrimental to cruise performance due to increased drag. For a given velocity decay requirement, the minimum number of elements for a multi-element nozzle appears to be obtained when the design value of $X\,(D_e\sqrt{1+M_j}\,)^{-1}$ is at the departure point of the coalescing core from the single element curve.

The preceding criteria could result in only a small number of elements for a given nozzle application. In turn, this could result in little, if any, jet exhaust noise reduction commonly associated with multi-element nozzles. Thus, from the point-of-view of jet exhaust noise reduction it may be desirable to use more elements and accept some small drag increase for the aircraft cruise condition.

Use of a mixer nozzle for reducing the jet-flap interaction noise from an externally blown flap in STOL aircraft applications must consider not only the effect of the reduction of the impinging velocity on the flap, but also the increased jet impingement area on the flap. This increased area is caused by the larger overall dimensions of the mixer-nozzle jet compared with that for a conventional circular-nozzle jet. Thus the full jet-flap interaction noise benefits resulting from the velocity decay associated with a mixer nozzle may be slightly reduced by the larger jet impingement area.

SYMBOLS

b, h, LR, r, s_r, W	nozzle dimensions (see Table I), cm
C_e	effective nozzle (or orifice) coefficient
D_e	effective diameter of circular nozzle with exit area equal to that of non-circular single element (D_e for a circular nozzle equals the nozzle diameter), cm
$D_{e,T}$	effective diameter of circular nozzle with exit area equal to that of total multi-element nozzle area, cm
M_j	jet Mach number
s/w	ratio of effective spacing between adjacent jets (including nozzle wall thickness) at nozzle exit plane to effective element width
U	local peak axial velocity of jet, m/sec
U_j	jet exhaust velocity, m/sec
U_b/U_c	ratio of bypass jet velocity to core jet velocity
X	axial distance downstream of effective nozzle exit plane
Subscripts	
0	center tube
1	first ring of multi-elements
2	second ring of multi-elements
0-1, 1-2	see Table I
i	inner
o	outer

REFERENCES

1. Dorsch, R. G., Krejsa, E. A. and Olsen, W. A.: Blown Flap Research. NASA TM X-67850, June 1971.

2. Higgins, C. C., and Wainwright, T. W.: Dynamic Pressure and Thrust Characteristics of Cold Jets Discharging from Several Exhaust Nozzles Designed for VTOL Downwash Suppression. NASA TN D-2263, April 1964.

3. Higgins, C. C., Kelly, D. P. and Wainwright, T. W.: Exhaust Jet Wake and Thrust Characteristics of Several Nozzles Designed for VTOL Downwash Suppression. NASA CR-373, January 1966.

4. Lee, R., et al: Research Investigation of the Generation and Suppression of Jet Noise. General Electric Co. (Prepared under Navy, Bureau of Weapons Contract NO as 59-6160-C.) January 16, 1961.

Table I

NOMINAL NOZZLE DIMENSIONS

Circular Tube-Type Nozzles

Nozzle Type	D_e, cm	$D_{e,T}$, cm	R_1, cm	R_2, cm	$(s/w)_1$,	$(s/w)_2$,	$s_{r_{0-1}}$, cm	$s_{r_{1-2}}$, cm
1-Tube	2.36	2.36	--	--	--	--	--	--
0-6-0*	↓	5.77	3.17	--	0.336	--	--	--
↓	↓	↓	3.81	--	.605	--	--	--
↓	↓	↓	5.04	--	1.14	--	--	--
↓	↓	↓	6.50	--	1.73	--	--	--
0-6-6	↓	8.18	5.04	10.8	1.14	3.3	--	1.14
0-6-12	↓	10.0	↓	10.8	↓	1.25	--	↓
1-6-0	↓	6.25	3.81	--	.605	--	.605	--
↓	↓	↓	5.04	--	1.14	--	1.14	--
↓	↓	↓	6.5	--	1.73	--	1.73	--
1-6-6	↓	8.5	3.17	6.35	.336	1.73	.336	.336
↓	↓	↓	3.81	7.62	.605	2.2	.605	.605
↓	↓	↓	5.04	10.8	1.14	3.3	1.14	1.14
1-6-12	↓	10.3	↓	↓	↓	1.25	↓	↓

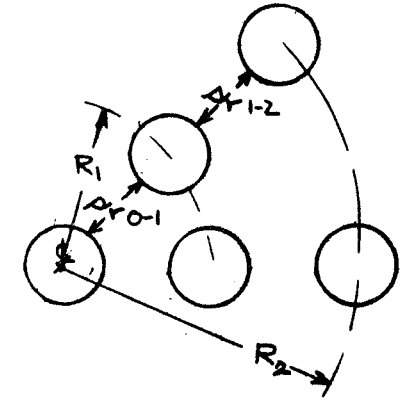

*Multitube nozzle designations: first number indicates whether center tube is used, second number indicates number of tubes in the first ring of tubes and third number indicates number of tubes in the second ring of tubes.

Rectangular Nozzles

Width, b, cm	Length, h, cm	Aspect Ratio
1.27	15.25	12
2.54	↓	6
5.08	↓	3
↓	7.62	1.5

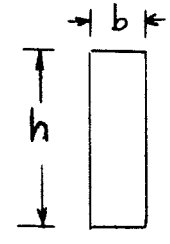

Triangular Nozzles

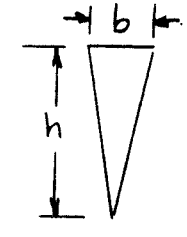

Base, b, cm	Altitude, h, cm
2.54	15.25
5.08	↓
↓	7.62

Table I (Continued)

NOMINAL NOZZLE DIMENSIONS

Trapezoidal Nozzles

(a) Square-ended

Number of Elements	D_e, cm	$D_{e,T}$, cm	h, cm	b_1, cm	b_2, cm	R_o, cm	s/w	r_i, cm	r_o, cm
12	2.23	7.75	3.17	0.86	1.63	3.17	1	--	--
1	↓	--	↓	↓	↓	--	---	--	--
6	3.17	7.75	↓	1.72	3.26	3.17	1	--	--
1	↓	--	↓	↓	↓	--	---	--	--
6	↓	7.75	5.23	0.89	2.23	3.17	3	--	--
1	↓	--	↓	↓	↓	--	---	--	--

(b) Round-ended

8	3.81	10.8	6.35	--	--	2.54	1.3	0.635	1.27
4	↓	7.62	↓	--	--	↓	3.6	↓	↓
1	↓	3.81	↓	--	--	--	---	↓	↓

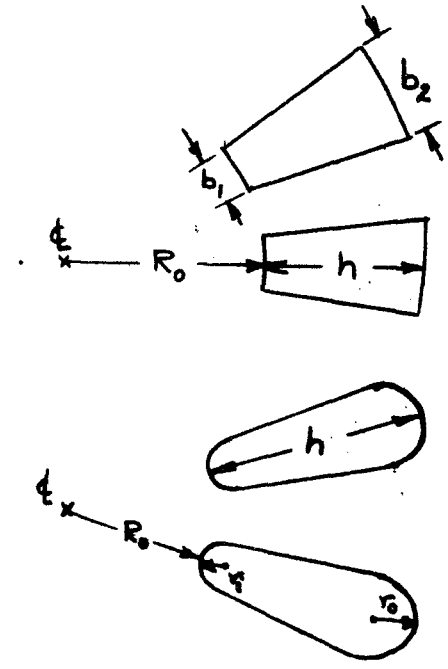

Non-Coplanar Nozzles

Number of Elements		D_e, cm		R_1, cm	L, cm	$(s/w)_1$	$(s/w)_2$	$s_{r_{1-2}}$, cm
Core	Bypass	Core	Bypass					
8	8	1.4	2.36	3.37	10.2	1.18	1.08	0.635
3	8	2.36	2.36	2.54	↓	0.84	↓	1.77

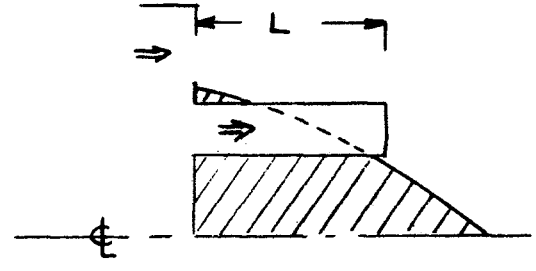

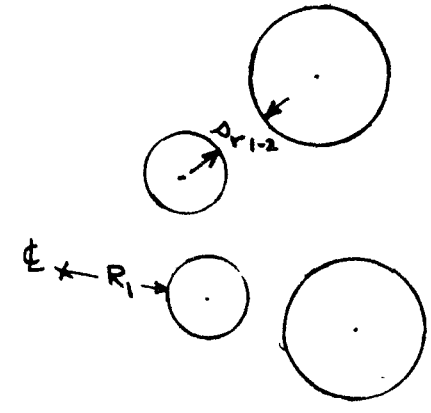

Table I (Concluded)

NOMINAL NOZZLE DIMENSIONS

Number of Elements		D_e, cm		Annulus	Core Tube	Annulus
Core	Bypass	Core	Bypass	height, cm	R_1, cm	R_1, cm
3	annulus	2.36	7.0	1.02	2.54	11.2
8	annulus	1.4	7.0	1.02	3.37	11.2

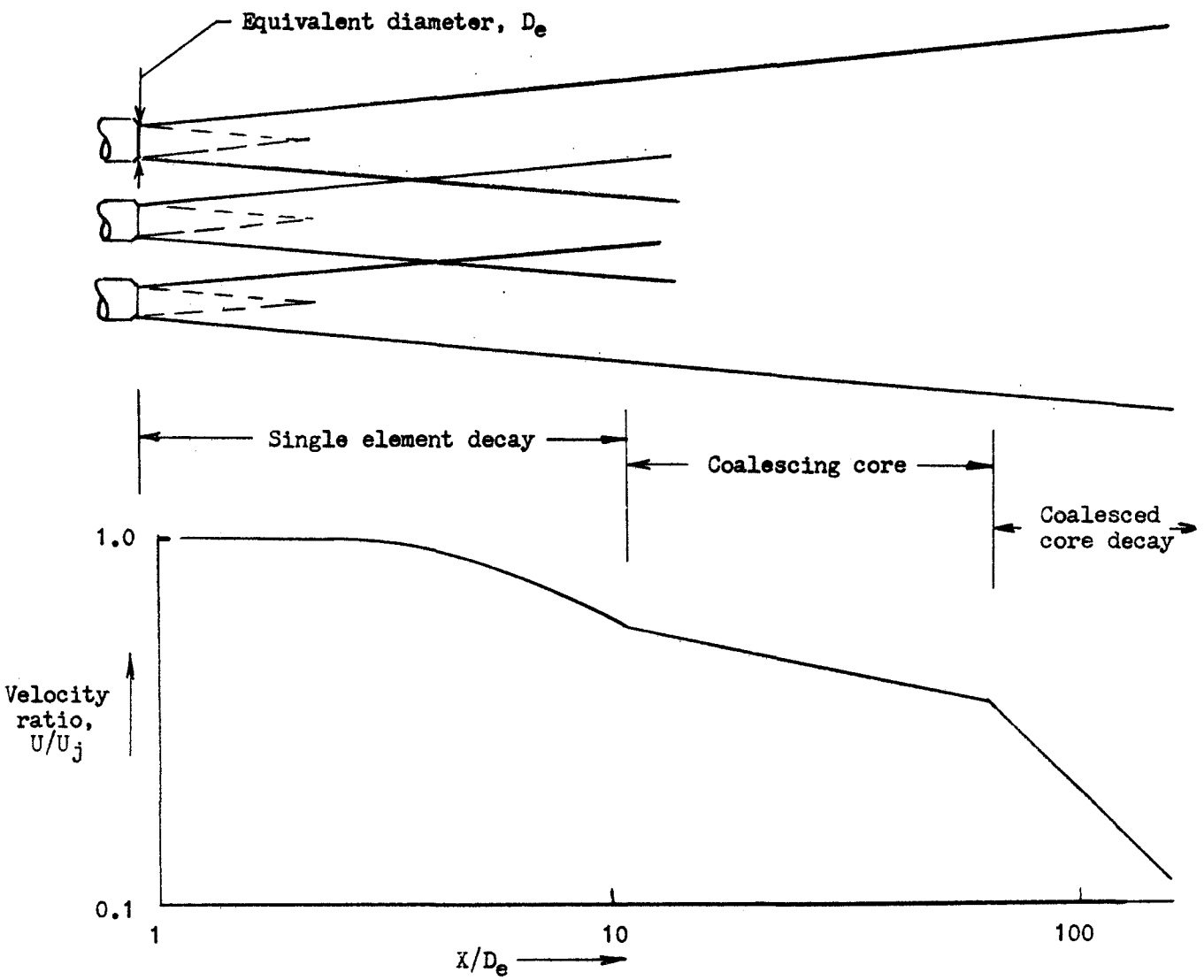

Figure 1.- Schematic representation of multi-element nozzle peak axial-velocity decay.

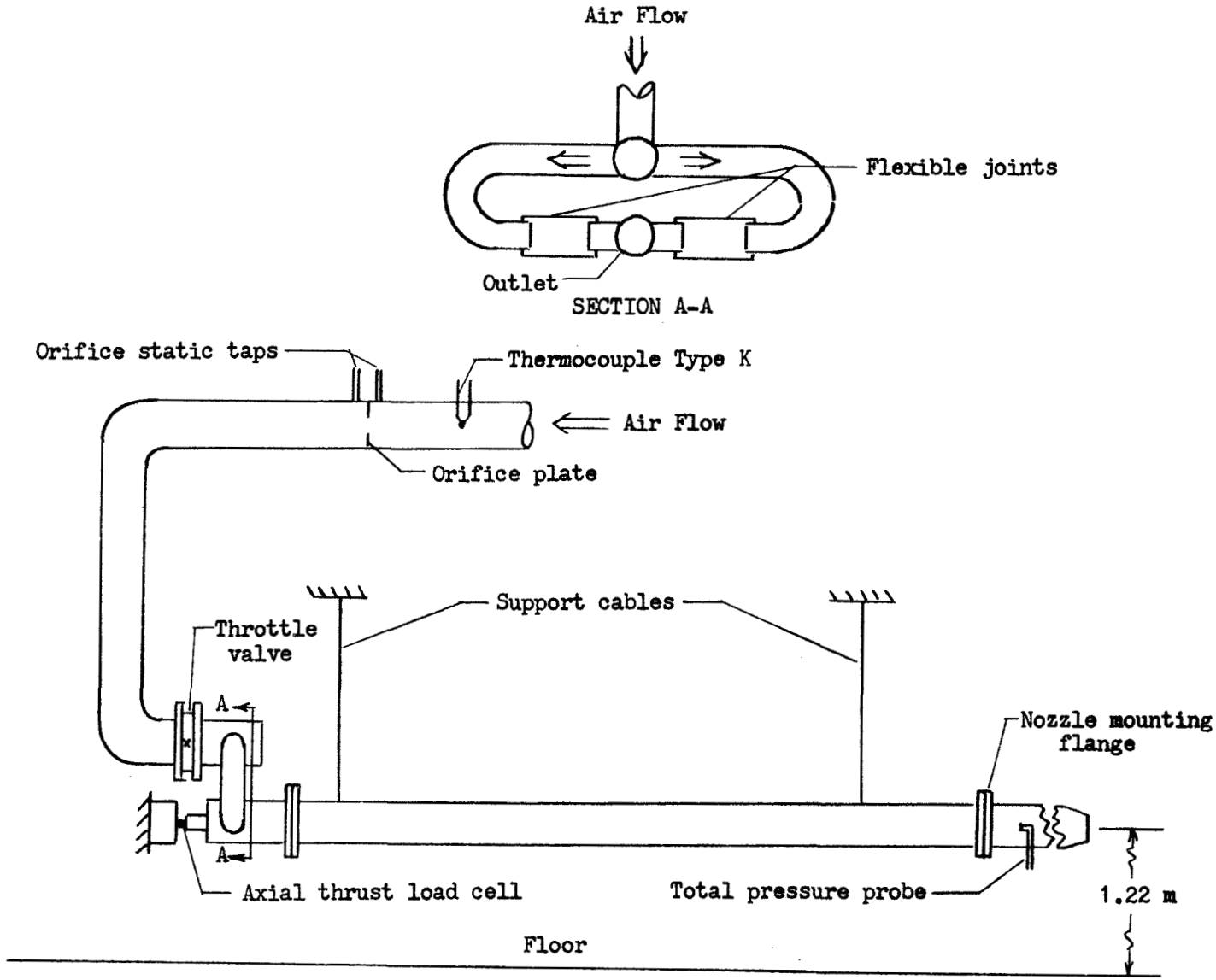

Figure 2.- Schematic diagram of test rig.

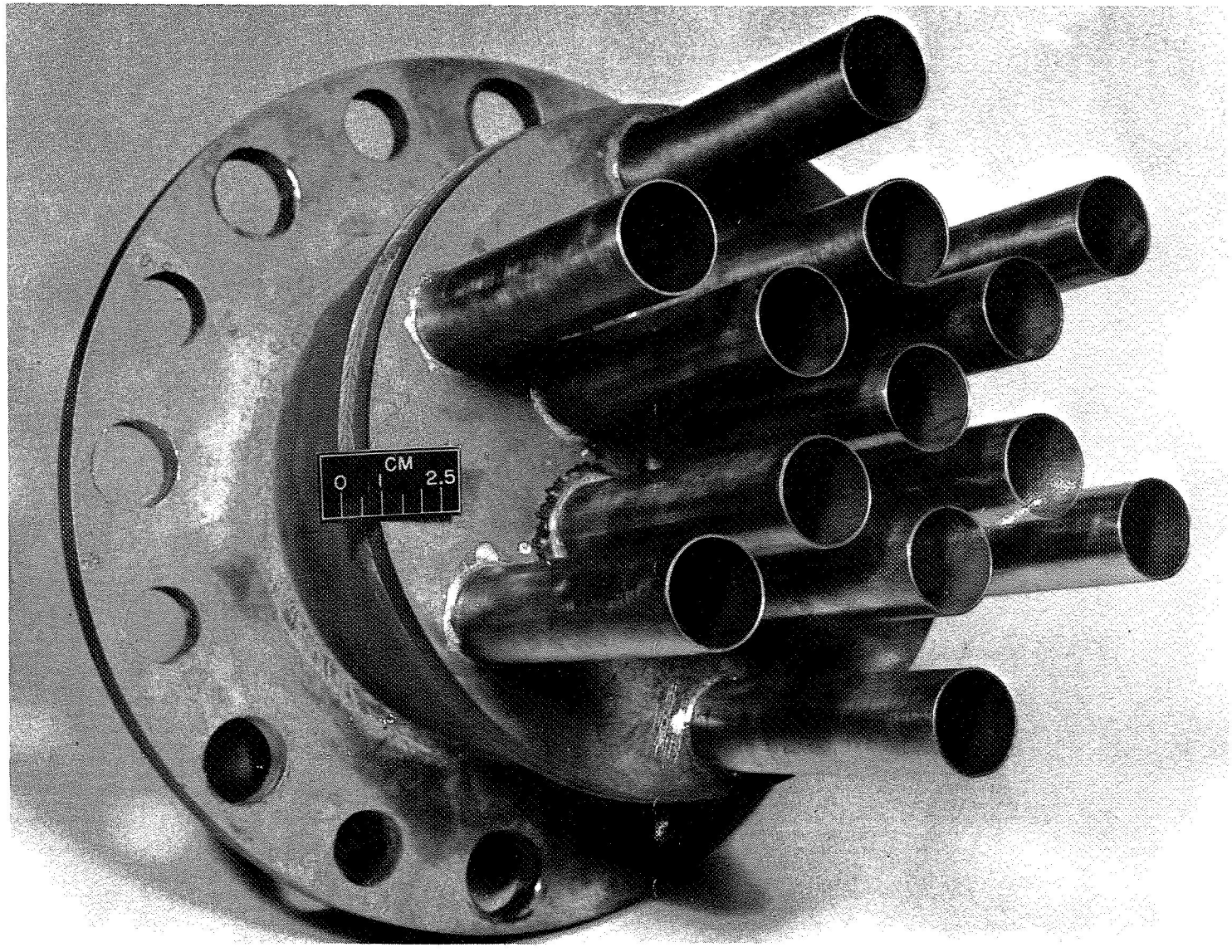

(a) Multitube nozzle.

Figure 3.- Typical multi-element nozzle configurations.

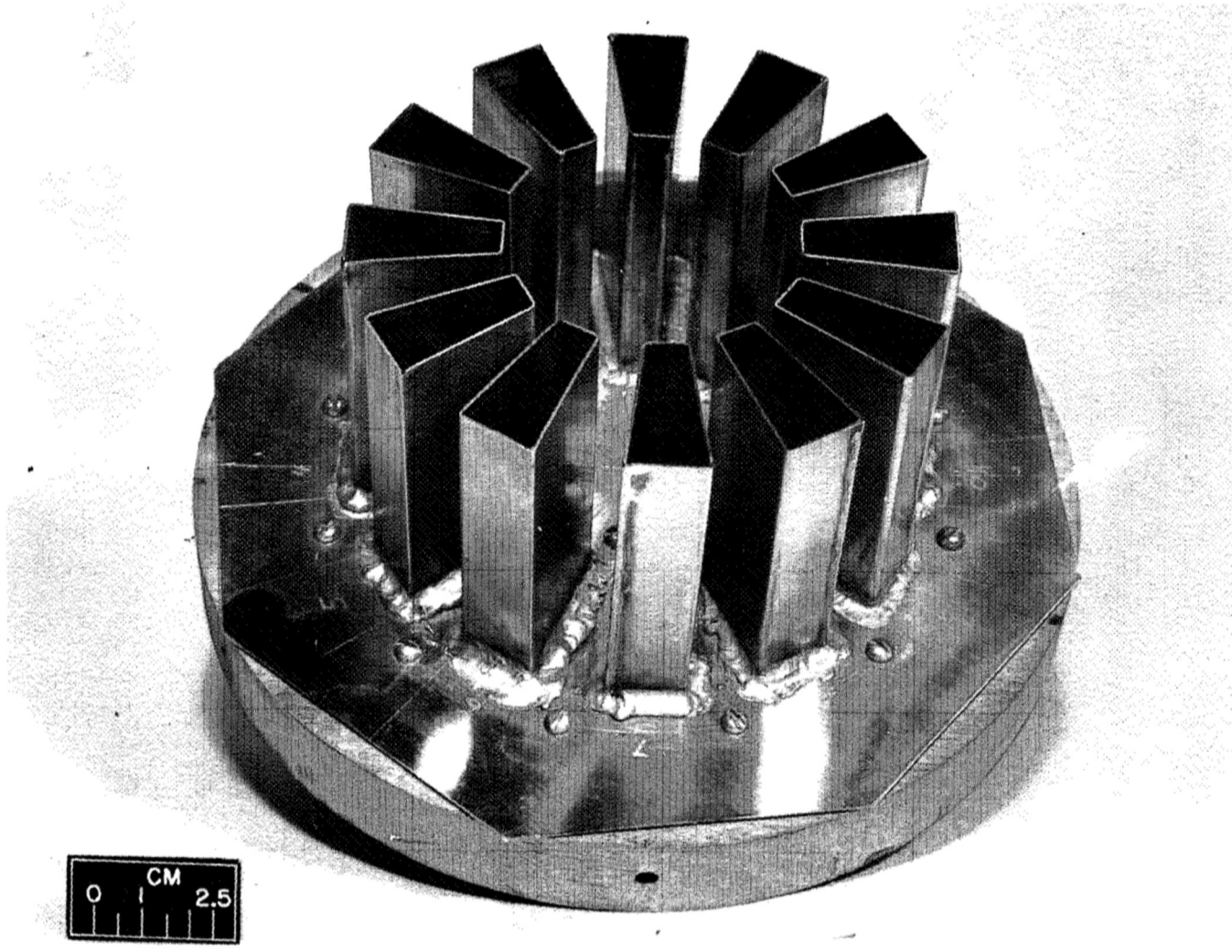

(b) Square-ended trapezoidal nozzle.

Figure 3 Continued.-

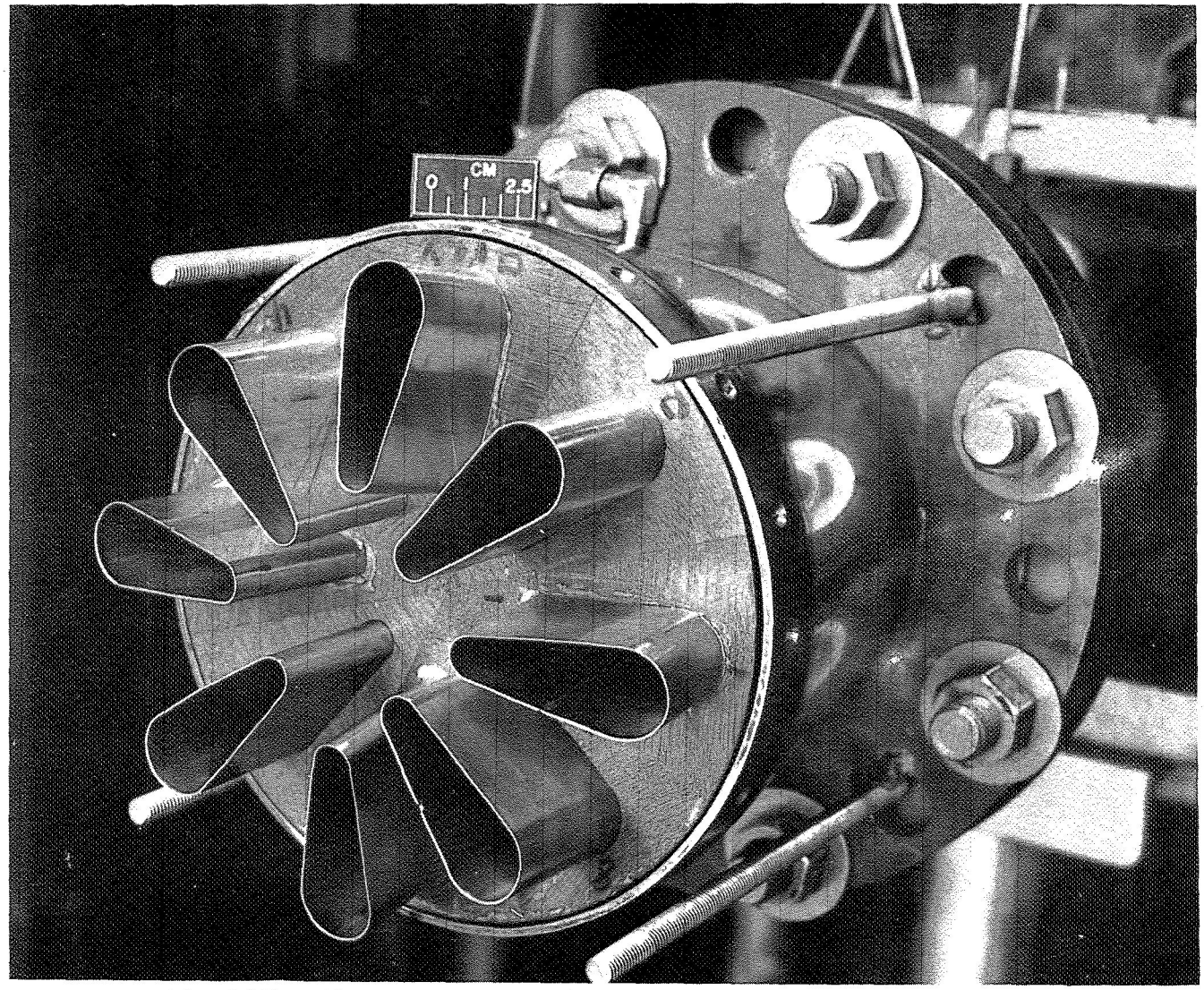

(c) Round-ended trapezoidal nozzle. Alternate lobes canted 10° outward from nozzle centerline.

Figure 3 Concluded.-

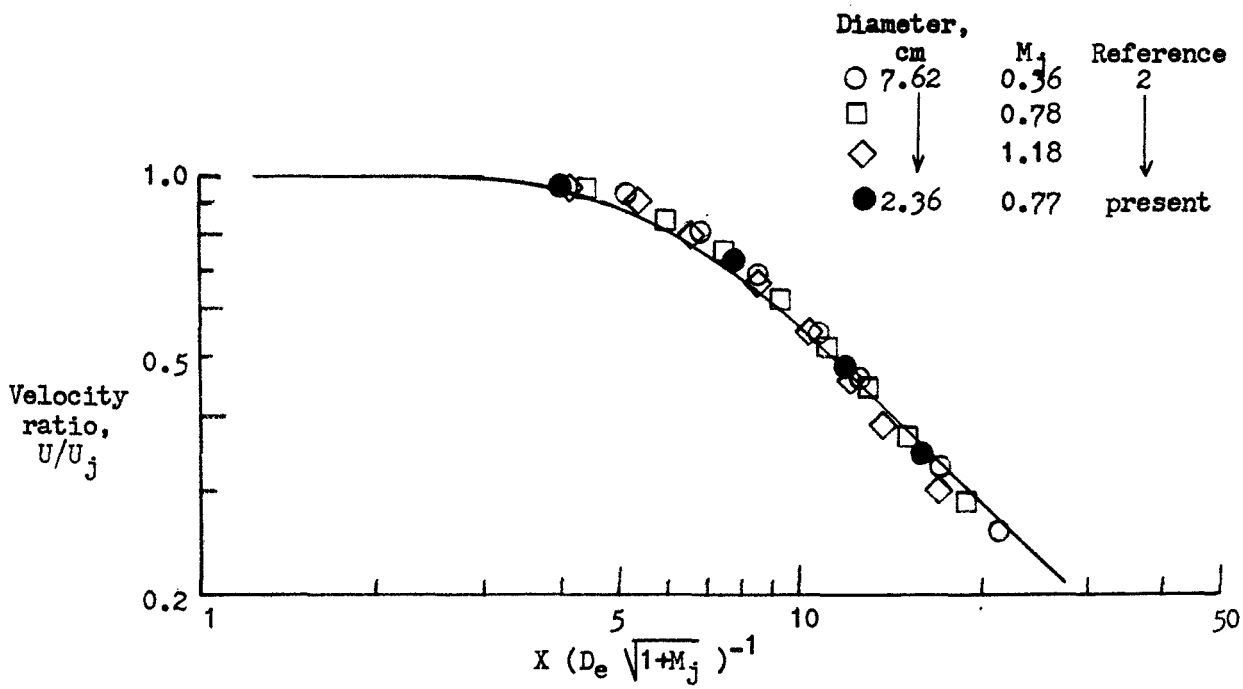

(a) Comparison of circular, convergent nozzle with circular-tube nozzle data.

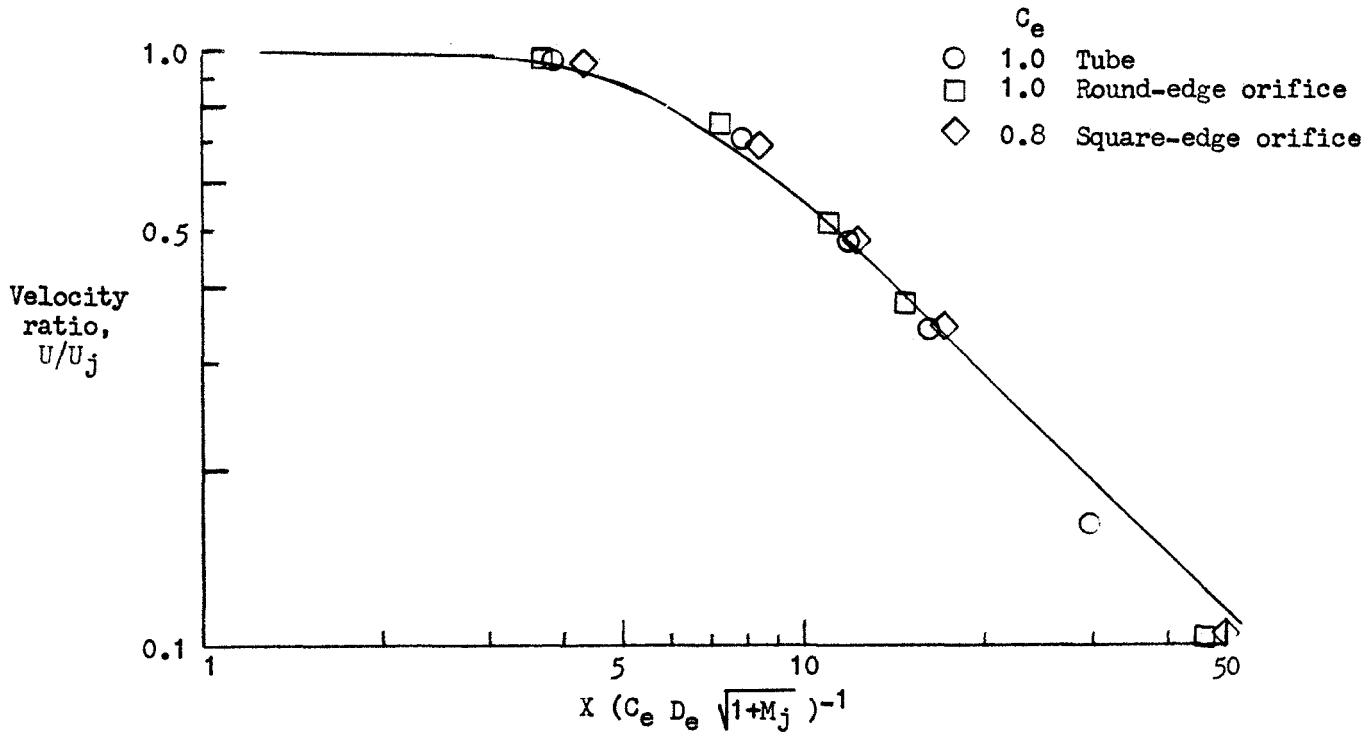

(b) Comparison of circular tube nozzle with circular orifice data. Element diameters, 2.36 cm. Nominal jet exit Mach number, 0.77.

Figure 4.- Peak axial-velocity decay obtained with circular single-element nozzles.

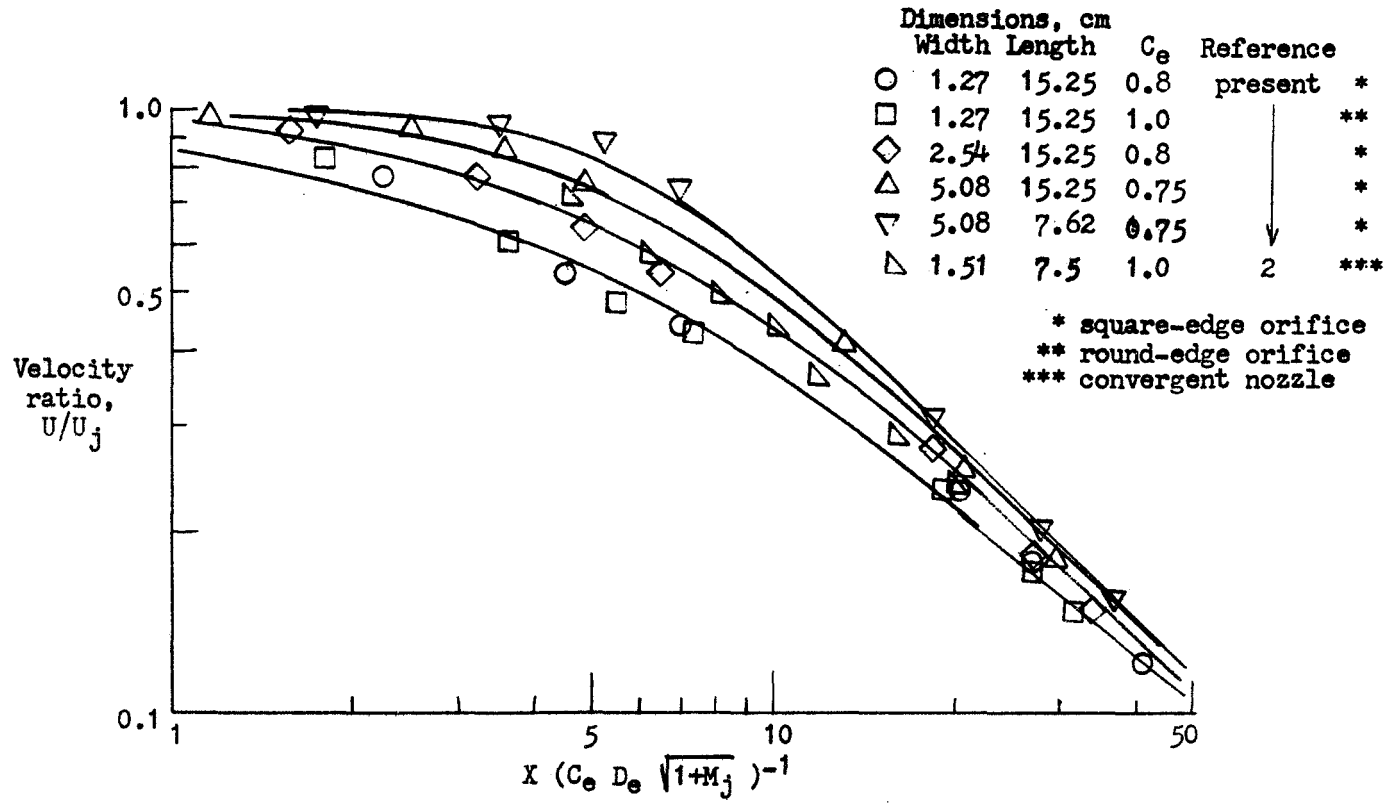

Figure 5.- Peak axial-velocity decay obtained with rectangular single-element nozzles. Nominal jet exit Mach number, 0.99

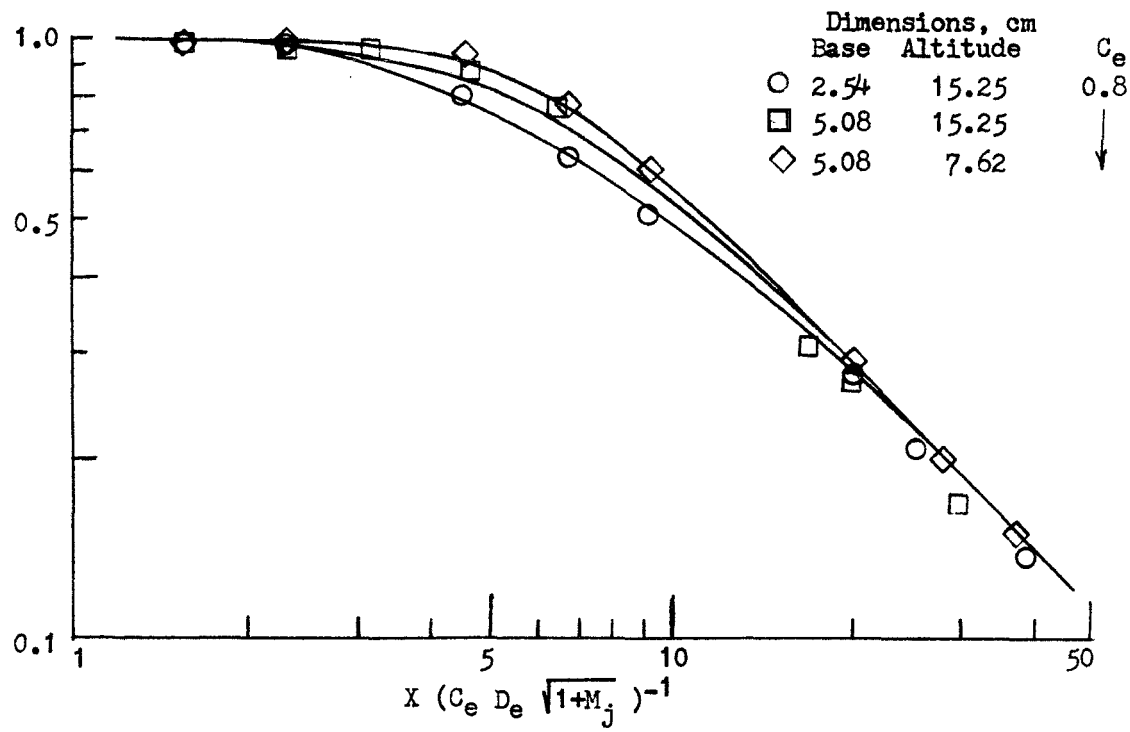

Figure 6.- Peak axial-velocity decay obtained with triangular single-element nozzles. Nominal jet exit Mach number, 0.99.

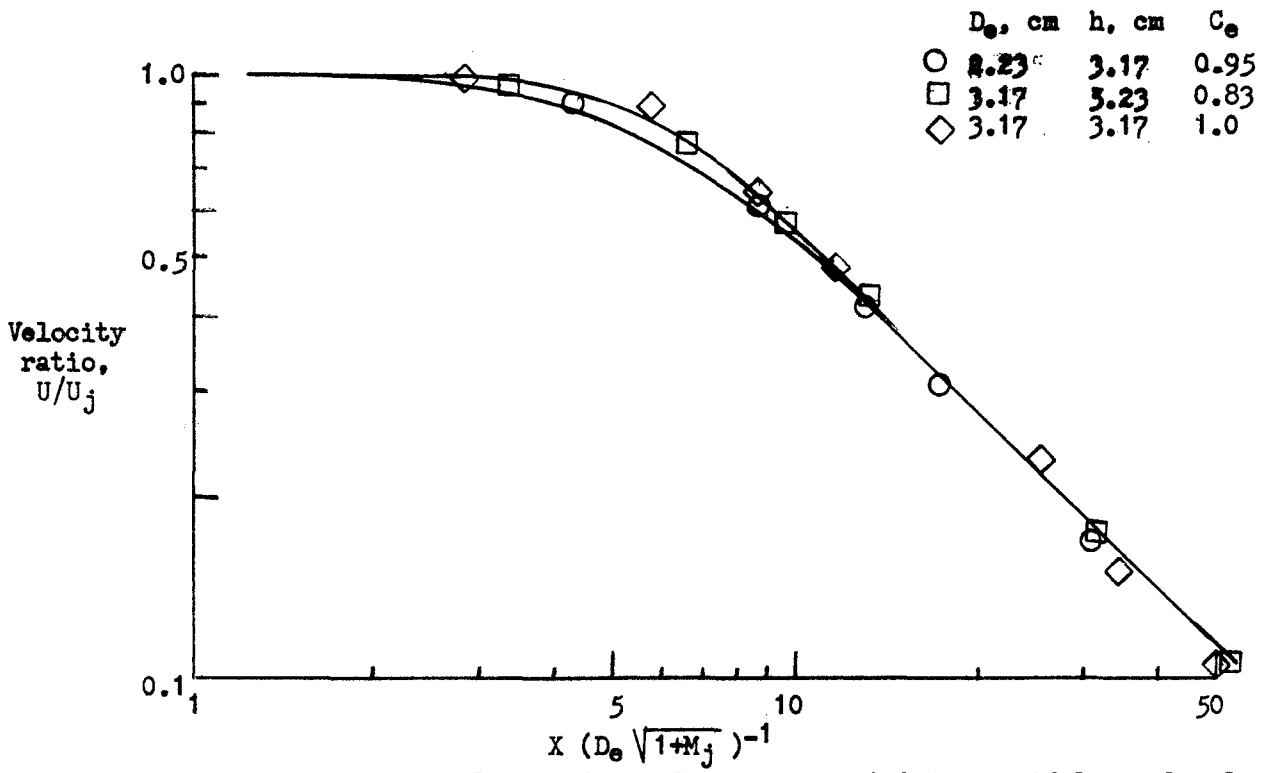

Figure 7.- Peak axial-velocity decay for square-ended trapezoidal, single-element nozzles. Nominal jet exit Mach number, 0.99.

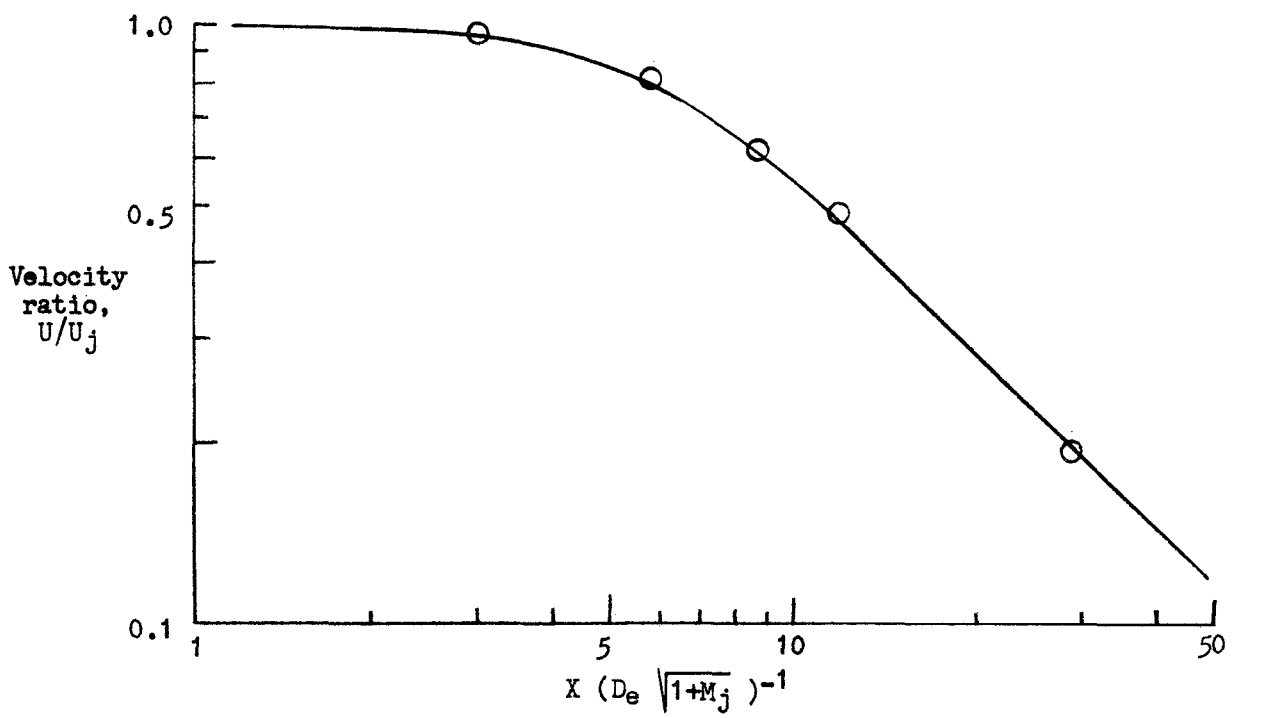

Figure 8.- Peak axial-velocity decay for round-ended trapezoidal, single-element nozzle. Nominal jet exit Mach number, 0.99; C_e = 1.0.

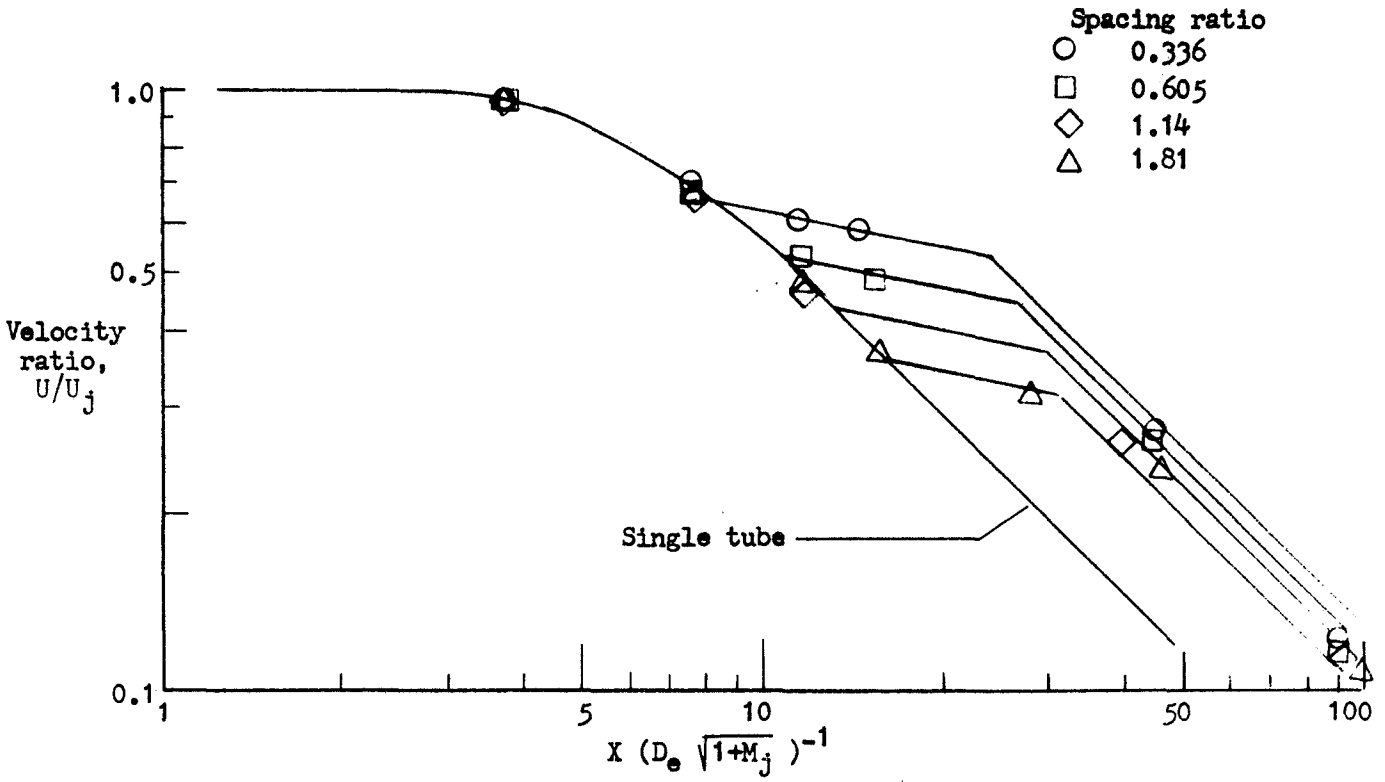

Figure 9.- Effect of element spacing on peak axial-velocity decay for a multitube (0-6-0) nozzle. Nominal jet exit Mach number, 0.99. Single tube diameter, 2.36 cm.

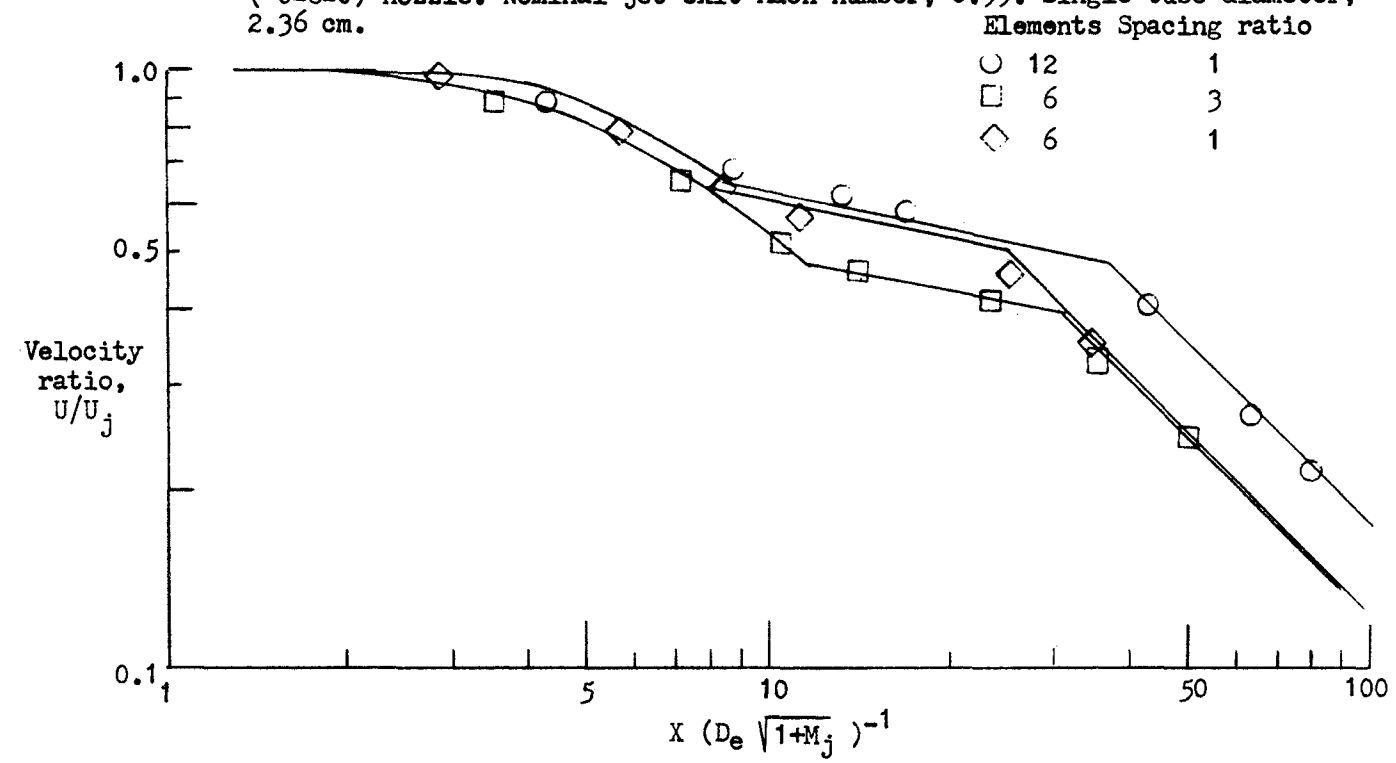

Figure 10.- Effect of element spacing and element number on the peak axial-velocity decay of square-ended trapezoidal nozzles. Constant total nozzle area, 47.5 cm^2; Nominal jet exit Mach number, 0.99.

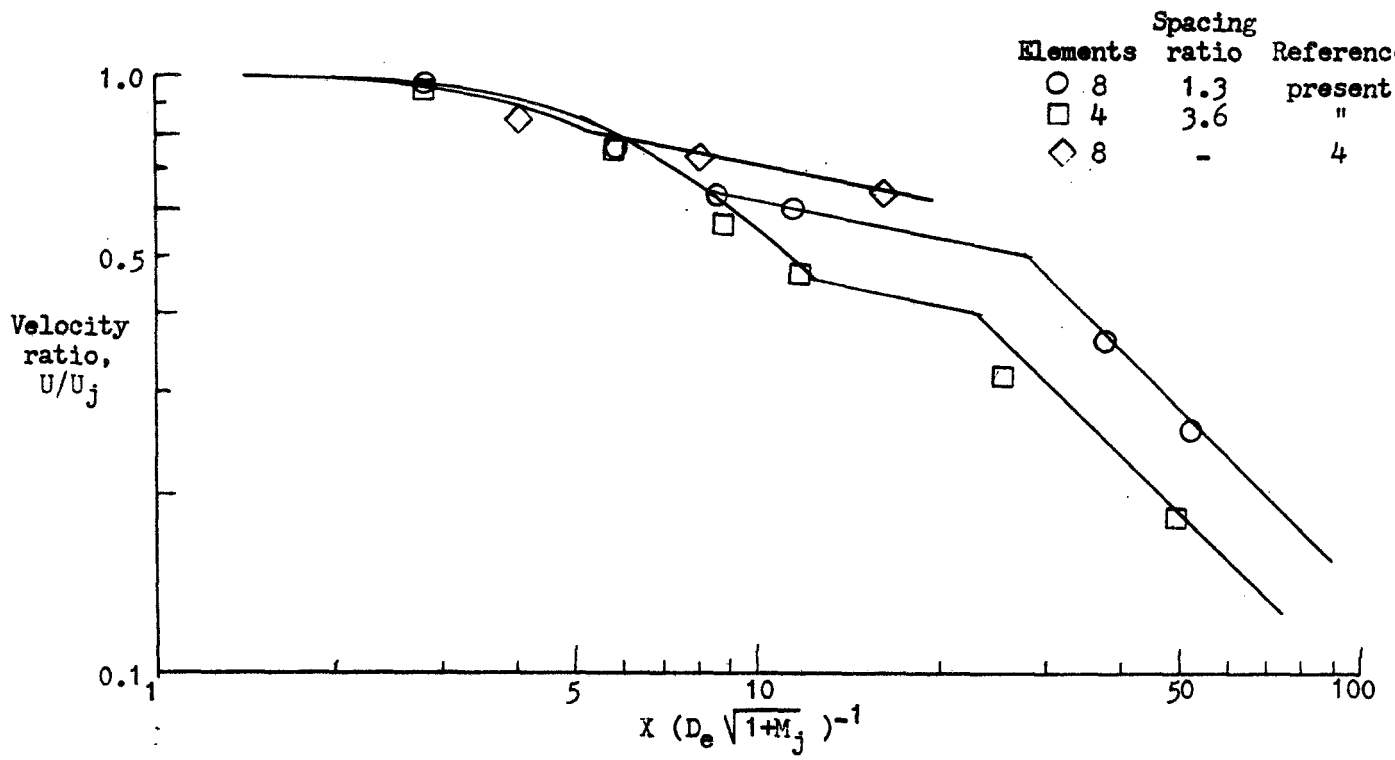

Figure 11.- Peak axial-velocity decay for several round-ended trapezoidal multi-element nozzles. Nominal jet exit Mach number, 0.99.

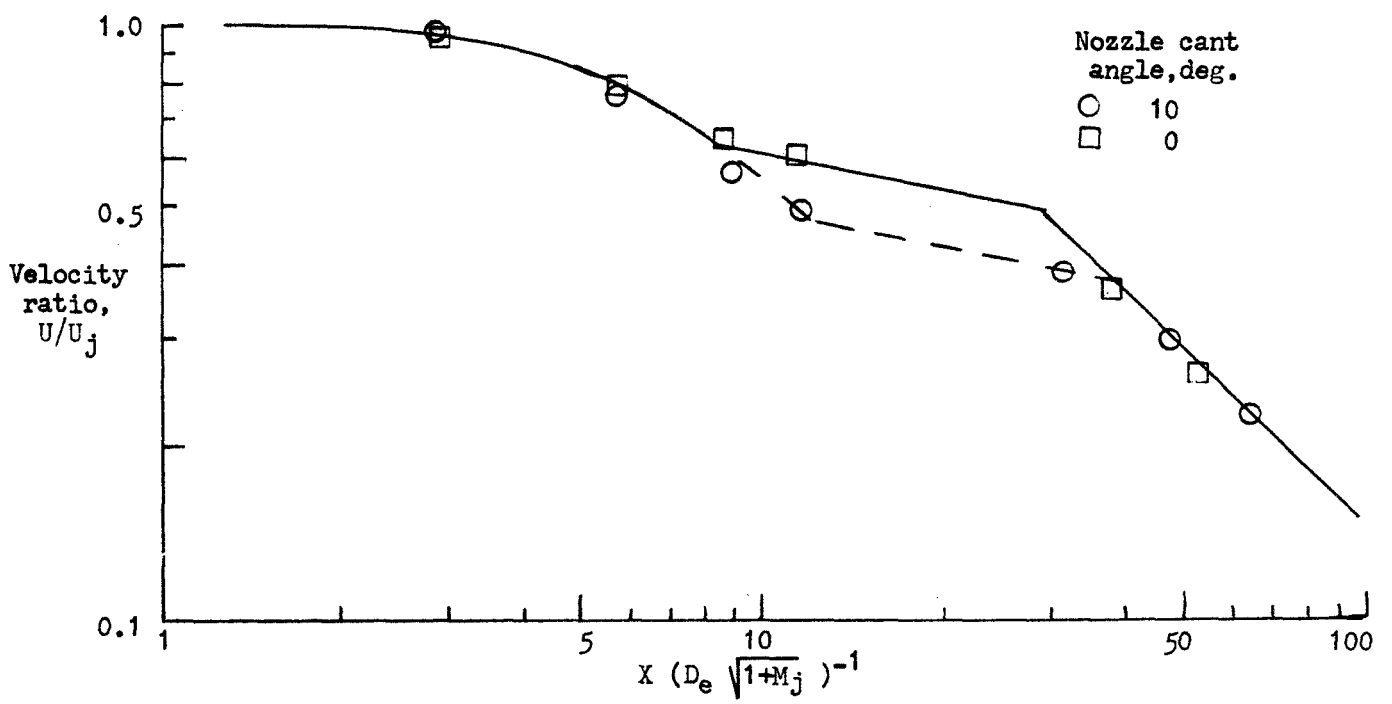

Figure 12.- Effect of canting alternate nozzles of an 8-lobe nozzle 10° outward from nozzle centerline. Round-ended trapezoidal elements. Nominal jet exit Mach number, 0.99.

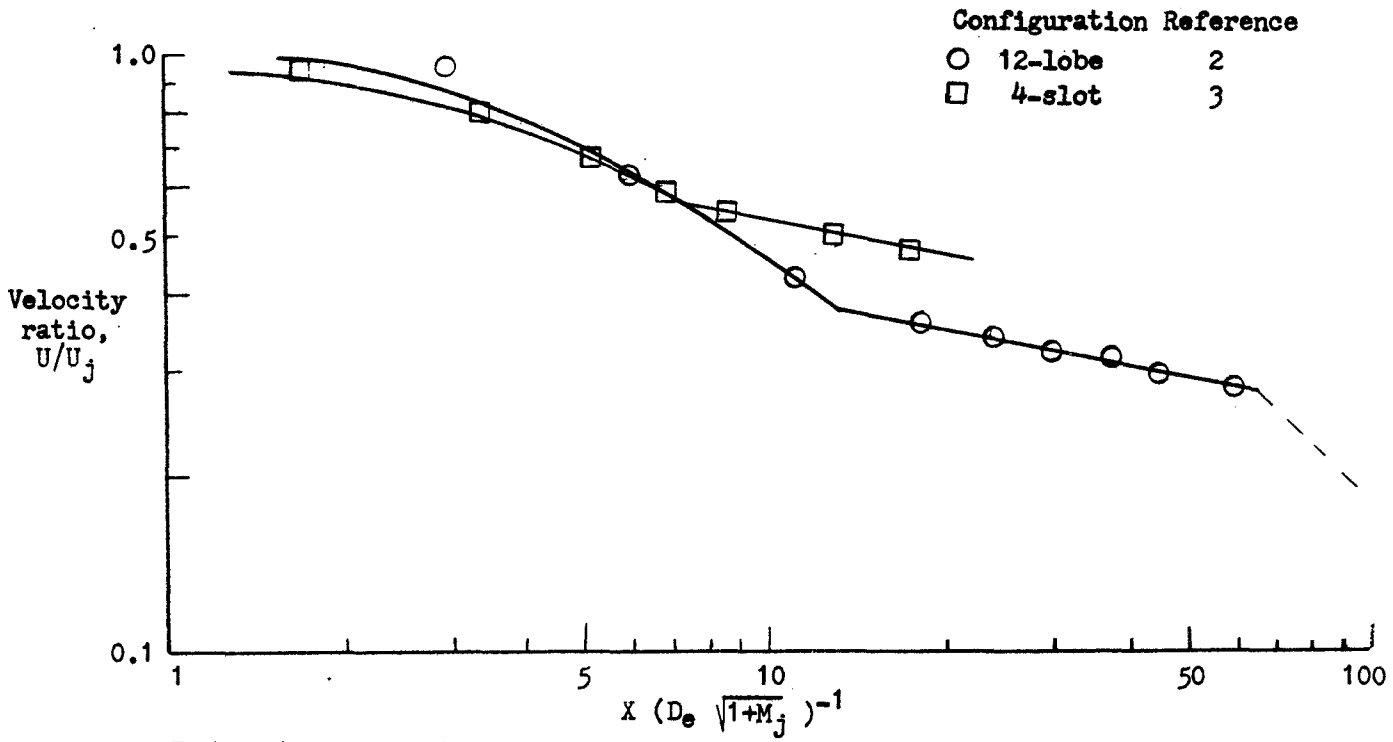

Figure 13.- Typical peak axial-velocity decay for two multi-element nozzles taken from the literature. Nominal jet exit Mach number, 1.05.

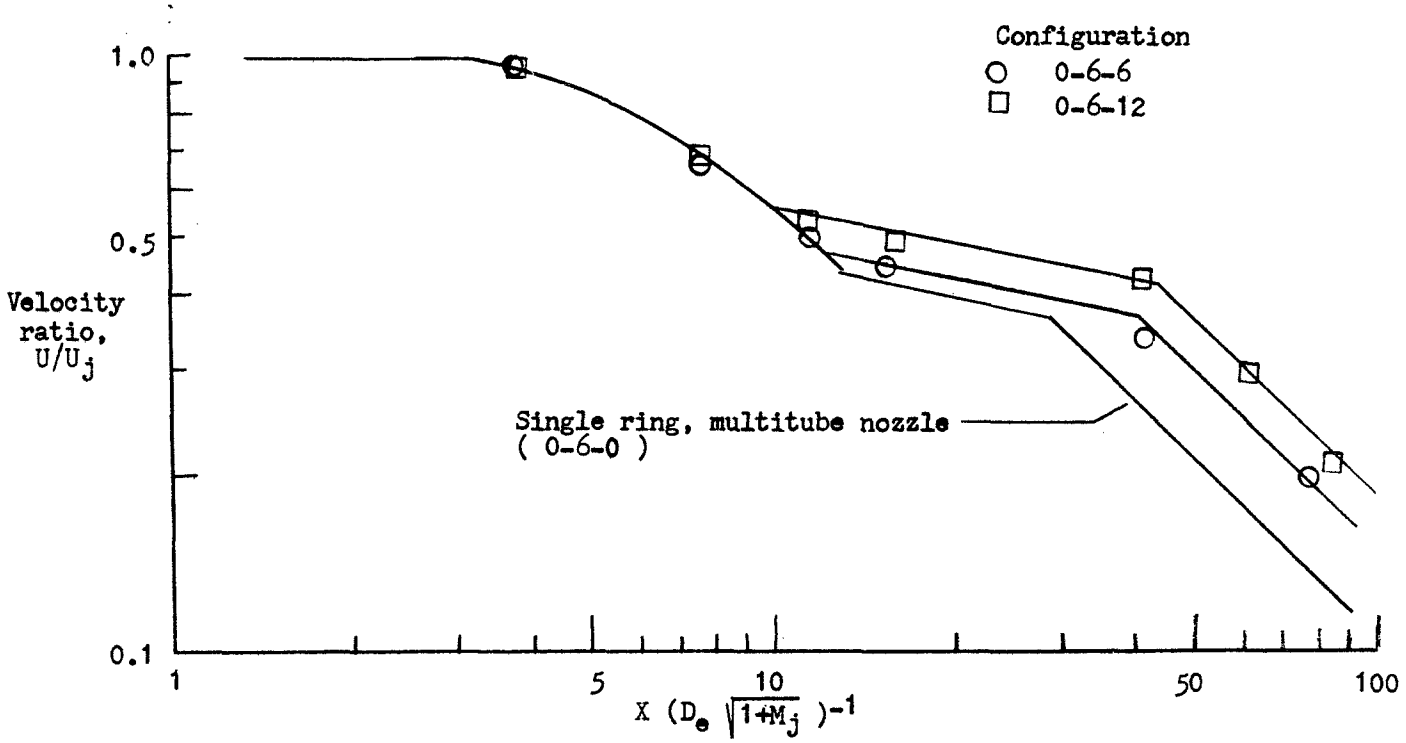

Figure 14.- Effect of muliple rings of multitubes on peak axial-velocity decay. No tube on nozzle centerline. Nominal jet exit Mach number, 0.99.

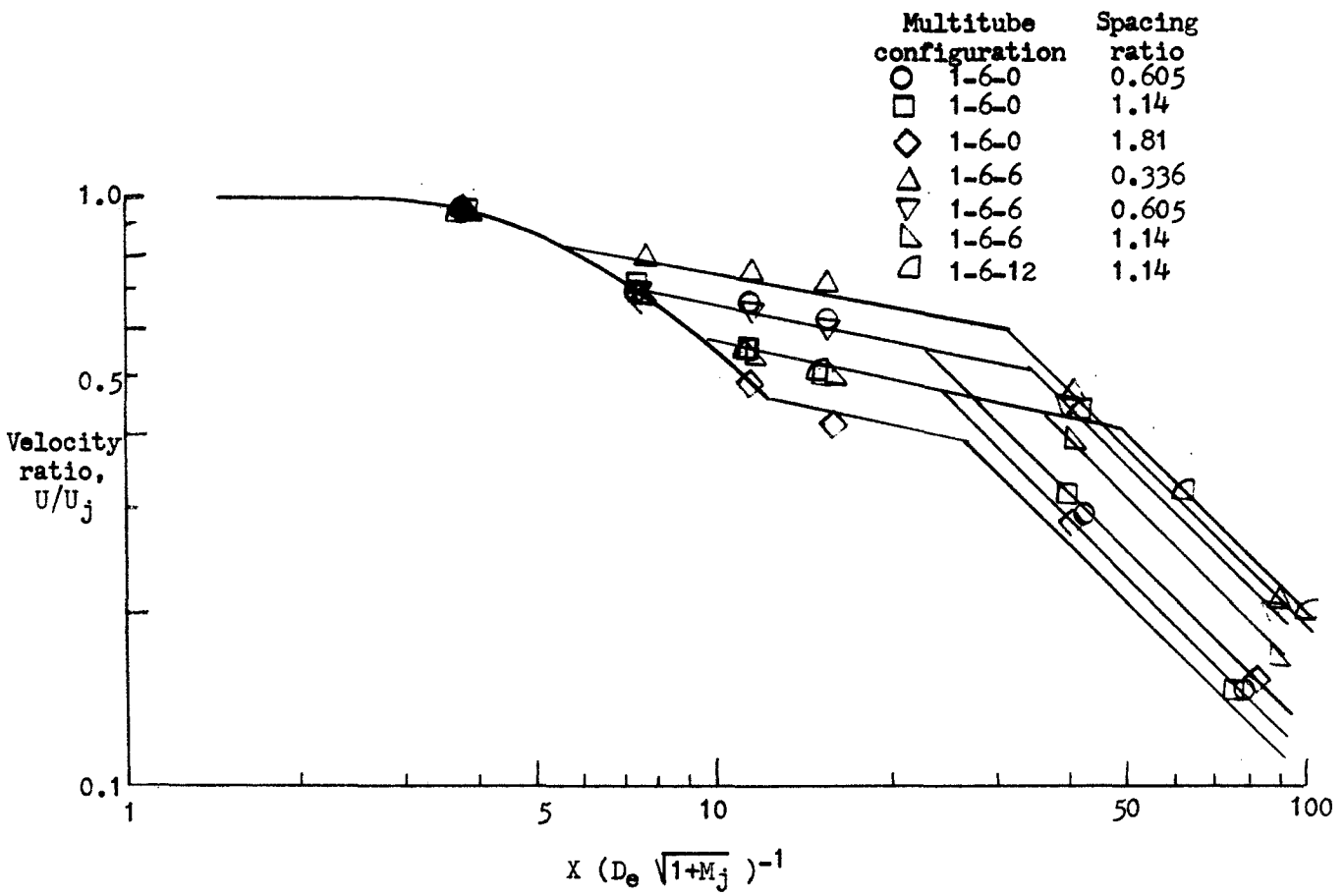

Figure 15.- Peak axial-velocity decay obtained with multiple rings of multitubes. Tube on nozzle centerline. Nominal jet exit Mach number, 0.99.

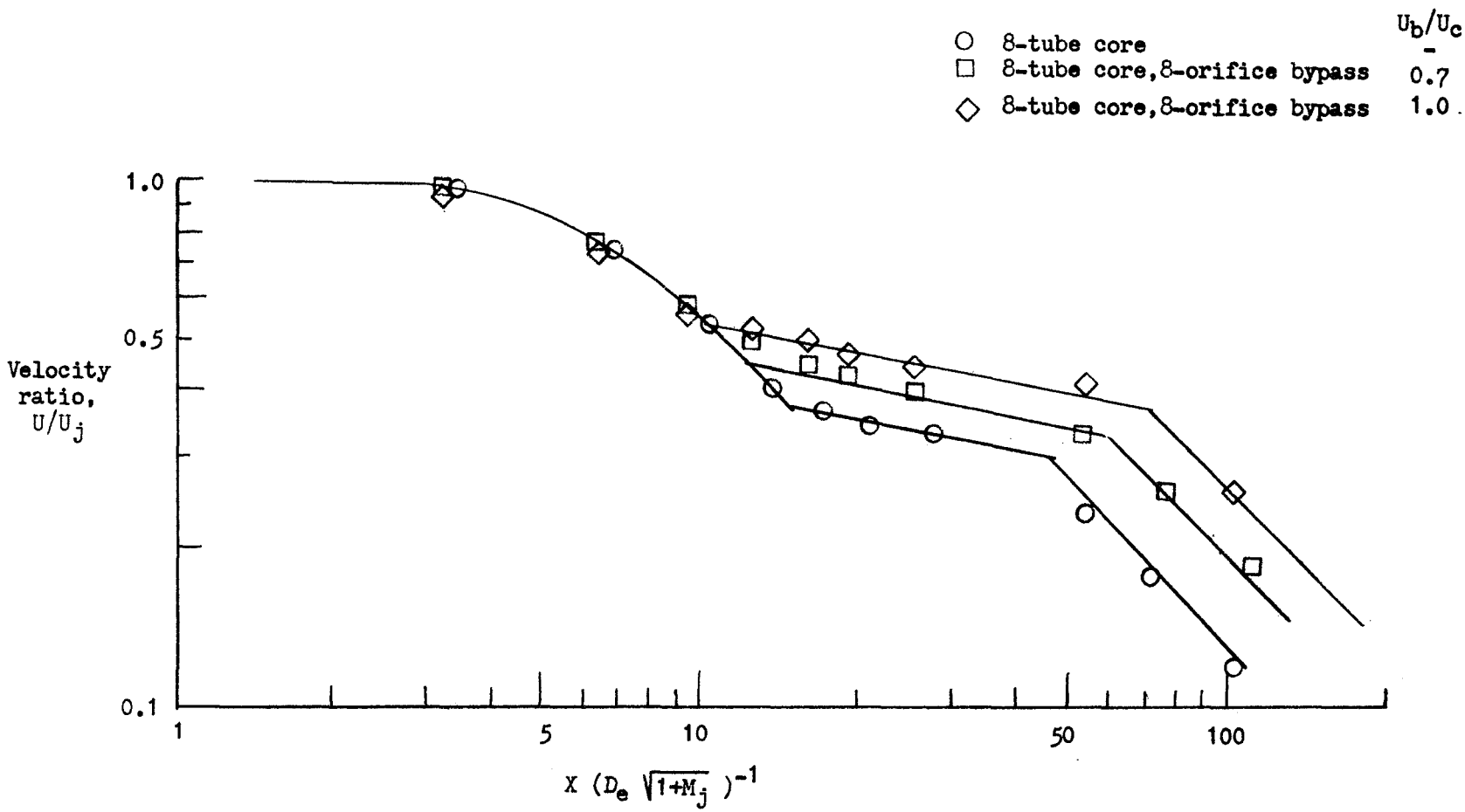

Figure 16.- Peak axial-velocity decay obtained with a nozzle having an 8-orifice bypass and an 8-tube core nozzle. Nominal core jet exit Mach number, 0.99

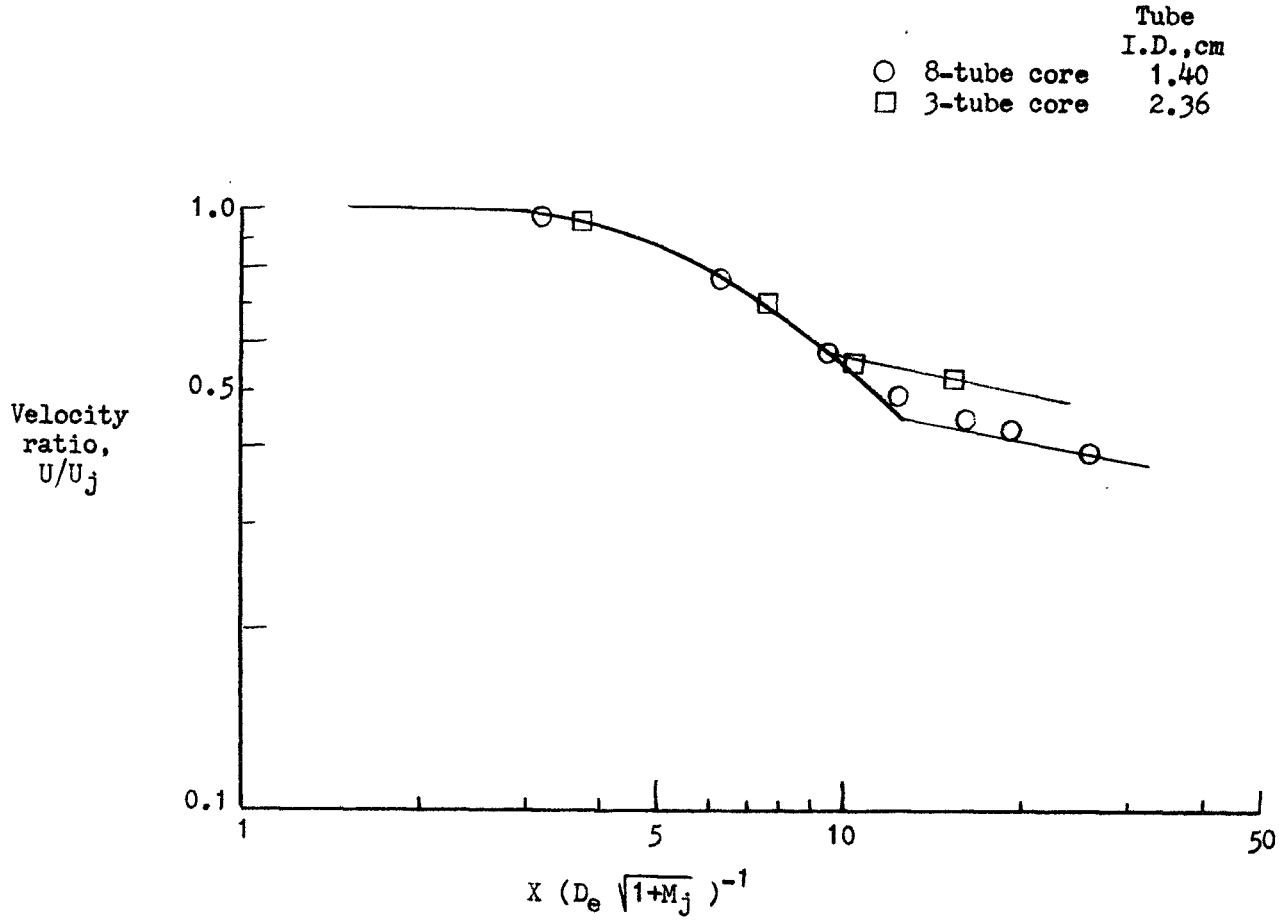

Figure 17.- Comparison of peak axial-velocity decay using an 8-orifice bypass nozzle with 3-tube and 8-tube core nozzles. Nominal core jet exit Mach number, 0.99; Single orifice diameter, 2.36 cm; Core- to bypass-plane axial distance, 10.2 cm. $U_b/U_c = 0.7$.

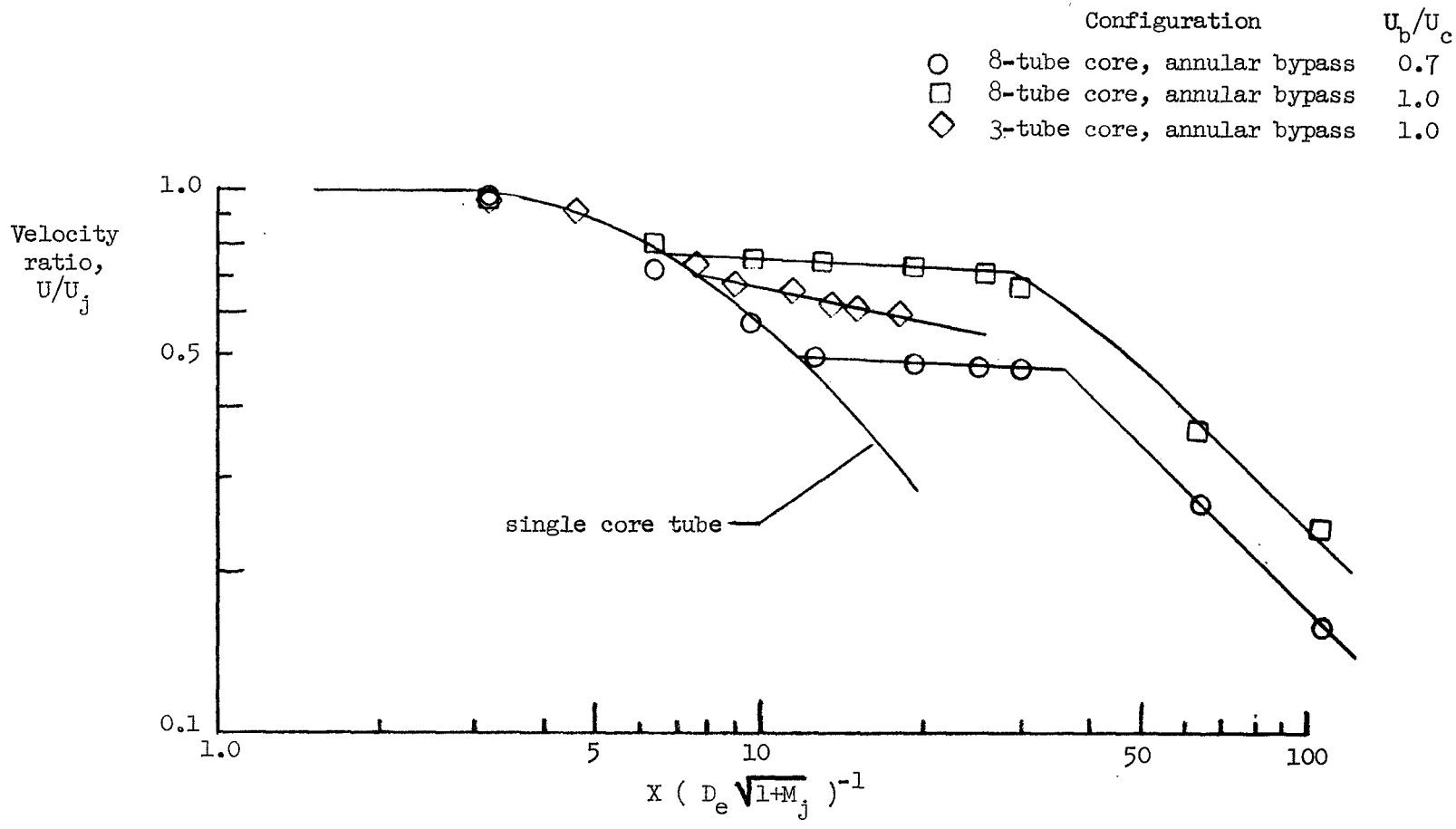

Figure 18. - Peak axial-velocity decay with nozzle having an annular bypass nozzle and a multitube core nozzle. Nominal core jet exit Mach number, 0.99.